

# Shear transmission on crack surface of ECC

T. Kanakubo

*University of Tsukuba, Tsukuba, Japan*

K. Shimizu

*Railway Technical Research Institute, Tokyo, Japan*

S. Nagai & T. Kanda

*Kajima Technical Research Institute, Tokyo, Japan*

**ABSTRACT:** In this paper, method of single plane shear test under tensile stress as normal stress on crack surface is conducted to clarify shear transfer mechanism on crack surface of ECC (Engineered Cementitious Composites). The PVA fiber is adopted for ECC. From the test results, shear strength on crack surface is about half of tensile strength. This means that normal stress for crack surface is possible to keep crack strength under shear. Predicting method for shear capacity of steel reinforced ECC beams is proposed based on the arch-truss method with the summation of the tensile strength of ECC which is obtained by bending test. The experimental values show good agreement with calculated values.

## 1 INTRODUCTION

High Performance Fiber-Reinforced Cementitious Composites (HPFRCC), which show the strain hardening branch and multiple cracking under uniaxial tensile stress, have been focused by lots of researchers because of its unique mechanical performance. Engineered Cementitious Composites (ECC) exhibit a maximum tensile strain of several percent owing to the synergetic effect of high-performance fiber and specifically designed mortar matrix. Unprecedented high-performance structural members can be expected when ECC is applied to seismic components.

It has been cleared that shear capacity of steel reinforced members using ECC subjected to earthquake force (bending - shear force) increases rather than ordinary steel reinforced concrete members (Shimizu 2004). It has been considered that tensile stress and shear stress can be transmitted through multiple cracks of ECC in the member as a result of the bridging action of high-performance fiber. However, shear transmission capacity of ECC can not be evaluated quantitatively because of difficulties of testing method and phenomenon itself. Though many uniaxial tension tests for ECC has been performed, the reports describing direct shear test for ECC are very limited.

In this paper, method of single plane shear test under tensile stress as normal stress on crack surface is conducted to clarify shear transfer mechanism on crack surface of ECC. The PVA fiber is adopted for ECC. Predicting method for shear capacity of steel

reinforced beams is proposed based on multiplying the reduction factor for tensile strength of ECC. The tensile strength of ECC is obtained experimentally from the evaluation of tensile properties using bending test result.

## 2 SINGLE PLANE SHEAR TEST

### 2.1 Loading method

Several testing methods for shear properties of ordinary concrete have been proposed. Some of these methods are shown in Figure 1. The shear test for concrete is categorized in two types; single plane shear test and double-plane shear test. Figure 1 shows the examples of single plane shear test. These test methods are utilized to investigate the shear properties of not only concrete but also reinforced concrete. In ordinary reinforced concrete specimens, crack width of crack surface is restricted by steel reinforcement and shear action is caused by bearing action by coarse aggregate and Dowel action by reinforcement. The controlled normal stress can be applied on crack surface when the testing method shown in the left figure is used.

In case of ordinary concrete, concrete itself does not carry tensile stress directly at crack surface after crack opening. It is considered that normal stress can be observed as the component force of bearing action of aggregate and Dowel action of reinforcement to perpendicular direction of crack surface.

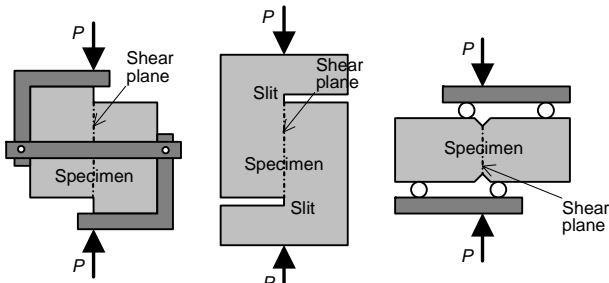


Figure 1. Examples of single plane shear test.

In case of HPFRCC, however, HPFRCC can carry tensile stress after cracking. And it is considered that tensile stress to perpendicular direction of crack surface and shear stress along the crack surface act by bridging action of fiber. Furthermore, it is very important to investigate shear transmission behavior for HPFRCC after crack opening. It seems to be difficult to observe these actions by using former mentioned testing method.

In this study, newly developed loading system is proposed to investigate direct shear properties of HPFRCC/ECC under tensile stress as shown in Figure 2. Shear force is applied as same as that shown in the right figure in Figure 1. The tensile force is subjected to the specimen directly using two oil jacks, which is separately controlled from applied shear force. The screw bolts embedded at the both ends of specimen are pulled via round surfaced loading devices. The rounded radius of the loading devices is decided to not restrict the displacement of the specimen due to shear force.

Before testing for ECC, the loading is conducted for ordinary reinforced concrete and mortar specimen in order to confirm the adaptability of this loading system. It is considered that no data exists previously for single plane shear test of reinforced concrete specimen under controlled tensile stress.

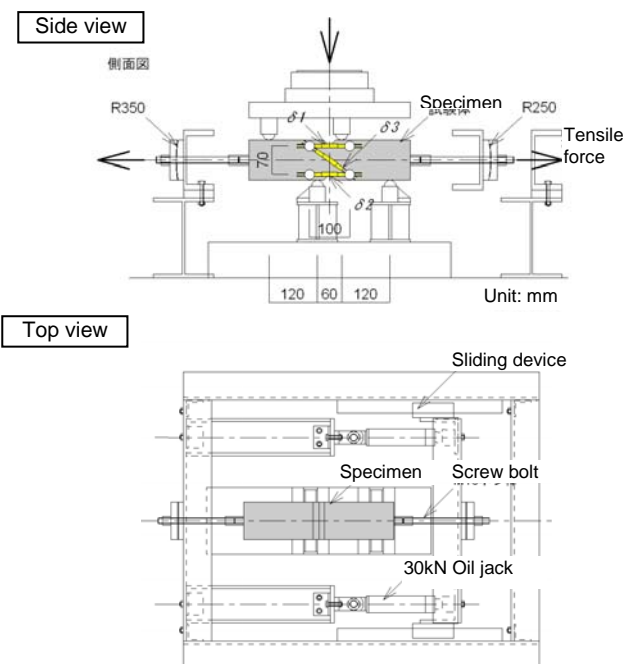


Figure 2. Loading system for single plane shear test.

## 2.2 Loading test for reinforced concrete

### 2.2.1 Specimen and materials

The reinforced concrete / mortar specimen for single plane shear test under tensile stress is shown in Figure 3. The sectional size is 100mm square. The notches are set at the central position of specimen and the dimension of shear plane is 70mm and 40mm for reinforced concrete specimen (NC) and mortar specimen (MT), respectively.

Four D4 reinforcements are embedded. The yield strength and tensile strength of D4 is 290MPa and 377MPa, respectively. Maximum size of coarse aggregate for normal concrete is 15mm. Compressive strength of normal concrete and mortar at the testing age is 30.0MPa and 50.6MPa, respectively.

The test parameter is the level of tensile stress. The tensile stress is kept constant through shear loading. The target tensile stress is from 0 to 14kN as the tensile force. The specimen identifications are indicated by the combination of the type of matrix (NC or MT) and the target tensile force (00 – 14).

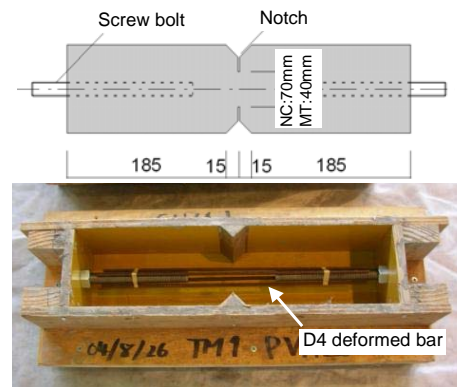


Figure 3. Reinforced concrete specimen and mold.

### 2.2.2 Test results

The crack patterns after loading are shown in Figure 4. In case of the lower level of tensile stress, compressive strut of the matrix is observed and cracks are formed diagonally between the loaded and supported position (MT08, NC08). In case of the higher level of tensile stress, on the other hand, one crack is formed at the center of specimen (MT14, NC14).

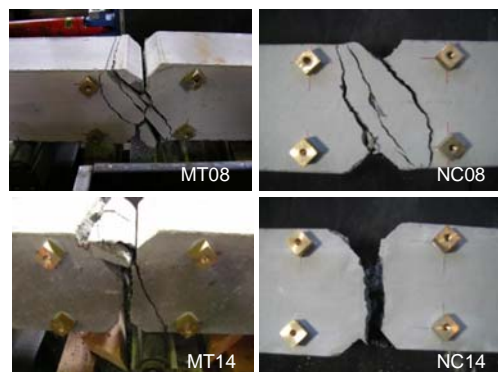


Figure 4. Crack patterns after loading.

Shear stress is measured by shear force divided by area of shear plane. Shear deformation and axial deformation are measured by displacement transducers which are set as shown in Figure 2. Shear stress versus axial deformation and shear deformation relationships are shown in Figure 5 and Figure 6. Both for NC specimens and MT specimens, the maximum shear stress decreases as the target tensile stress increases. And the deformation at maximum stress increases as the target tensile stress increases.

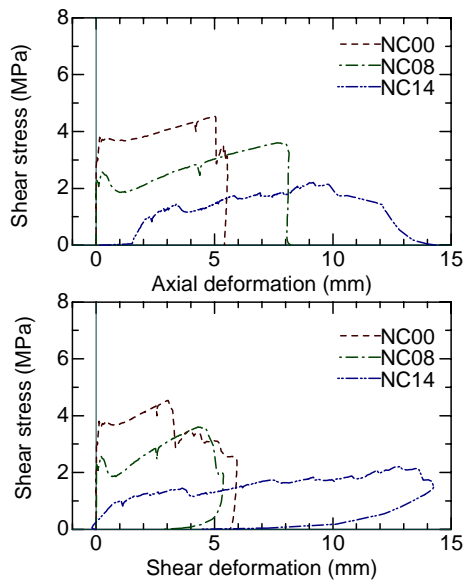


Figure 5. Shear stress – deformation relationship for NC specimen.

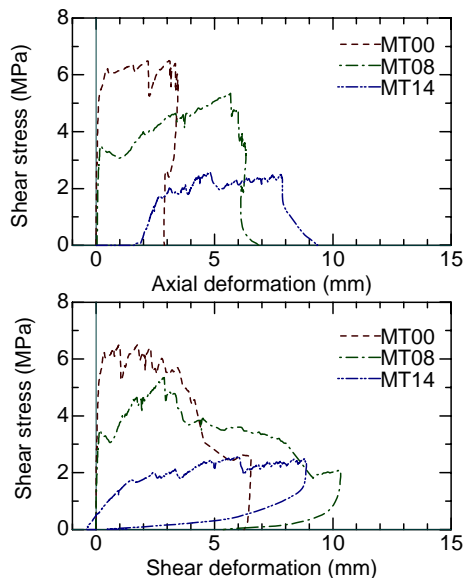


Figure 6. Shear stress – deformation relationship for MT specimen.

The measured maximum shear stress is compared with evaluation method proposed previously. Equation (1) (Mattock & Hawkins 1972) and Equation (2) and (3) (Li & Maekawa 1990) have been proposed by single plane shear test results. However, these tests were done under compression normal stress. Equation (1) has been proposed by regression

analysis from test results. Equation (2) and (3) have been introduced by considering contact behavior of crack surface and the probability of roughness of crack surface. The Dowel action has not been involved in Equation (2) and (3).

$$v_u = 1.38 + 0.8(p \cdot f_y + \sigma_N) \quad (1)$$

$$p \cdot f_y + \sigma_N = m \cdot \left[ \frac{\pi}{2} - \tan^{-1} \left( \frac{m - v_u}{v_u} \right)^{0.5} - \frac{\left( \frac{m - v_u}{v_u} \right)^{0.5}}{1 + \frac{v_u}{m - v_u}} \right] \quad (2)$$

$$m = 3.826 f_c^{\frac{1}{3}} \quad (3)$$

where  $v_u$  = shear strength;  $p$  = reinforcement ratio;  $f_y$  = yield strength of reinforcement;  $\sigma_N$  = normal stress (compression is positive); and  $f_c$  = compressive strength of concrete.

Figure 7 shows the relationships between observed test results for NC and MT specimens and calculated shear strength. Though specimens tested in this study are subjected under tensile stress, calculation value by Equation (2) well evaluates test results. The calculation value underestimates test result in the region of higher tensile stress (lower  $p f_y + \sigma_N$ ). It is considered that Dowel action which is ignored in Equation (2) relatively becomes larger rather than contact action in this region.

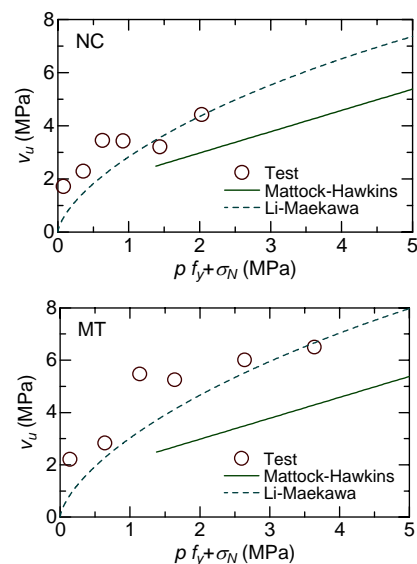


Figure 7. Comparison of maximum shear stress.

## 2.3 Loading test for ECC

### 2.3.1 Specimen and materials

The ECC specimen for single plane shear test under tensile stress is shown in Figure 8. The sectional size is 100mm square. The notches are set at the central position of specimen and the dimension of shear plane is 70mm.

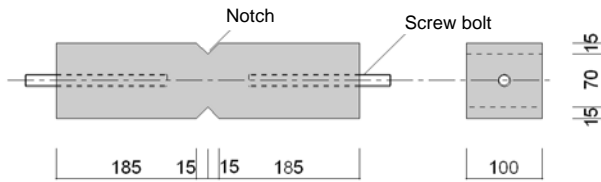


Figure 8. ECC specimen.

Polyvinyl alcohol (PVA) fiber shown in Table 1 is utilized for ECC. The volume fraction of PVA fiber is set to 1.5% (PVA15) and 2.0% (PVA20). Mix proportion of PVA-ECC is shown in Table 2. Moderate-heat Portland cement and fly ash (type II by JIS A 6201) are used as binder. Crushed limestone which specific surface area is  $2500\text{cm}^2/\text{g}$  is used as the fine aggregate. PVA-ECC was mixed by using a practical mixer with volume of  $1\text{m}^3$ . The specimens were uniformly and continuously cast into the mold. After steam curing for 8 hours with 35 Celsius degree, the specimens were cured in atmospheric environment.

Mechanical properties of PVA-ECC are shown in Table 3. Cylinder type test pieces with  $100\phi\text{-}200\text{mm}$  size are used for compression test. To determine the tensile characteristics of HPFRCC, lots of direct tension test methods have been proposed (Kanakubo 2006). Tensile characteristics of HPFRCC are considered to be sensitive by boundary condition and size and shape of specimen. Japan Concrete Institute (JCI) Standard (JCI-S-003-2007) gives one of the simple methods of reverse calculation from bending characteristics to tensile ones. The assumption of stress distribution for pure bending region indicated in JCI Standard is shown in Figure 9. The ultimate strain ( $\varepsilon_{tu,b}$ ) and tensile strength ( $f_{t,b}$ ) can be obtained from the maximum moment and curvature by the bending test results by easy calculation. In this study, ultimate strain of PVA20 and PVA15 is 1.07% and 0.42%, respectively. However, it is considered that PVA15 does not show strain-hardening behavior in uniaxial tension test.

Table 1. Properties of PVA fiber.

Fiber Type	Fiber length (mm)	Diameter (mm)	Tensile strength (MPa)	Elastic modulus (GPa)
PVA	12	0.04	1600	40

Table 2. Mix proportion of PVA-ECC.

Water by binder ratio	Sand by binder ratio	Air content (%)	Fiber vol. fraction (%)
0.42	0.77	10	1.5, 2.0

Table 3. Mechanical properties of PVA-ECC.

ID	Compression		Tension *	
	Elastic Modulus (GPa)	Comp. strength (MPa)	Tensile strength (MPa)	Ultimate strain (%)
PVA20	16.7	42.5	4.79	1.07
PVA15	16.2	40.1	2.41	0.42

\* Calculated value from bending test results (JCI-S-003-2007)

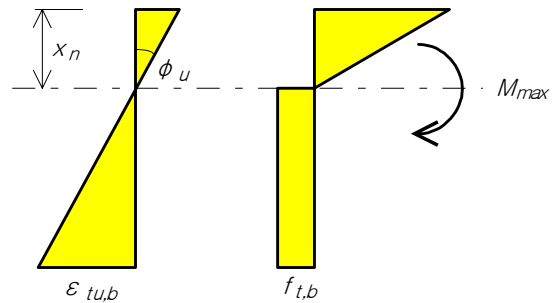


Figure 9. Stress distribution assumption in JCI-S-003-2007.

### 2.3.2 Loading method

In case of reinforced concrete specimen, tensile stress is kept constant as the target level. In case of ECC, however, tensile stress which is carried by fiber after first cracking differs by each specimen. Moreover, axial deformation (crack opening) at the same tensile stress is different. For loading of ECC specimens, the target is set to axial deformation. The tensile stress is kept constant when the axial deformation reaches the target deformation ( $w_{exp}$ ) after first cracking in the pre-loading only by tensile force. After that, shear load is applied to the specimen under constant tensile stress. As a result, level of tensile stress differs by each specimen. It can be said that the tensile stress kept constant is similar level of crack strength.

### 2.3.3 Test results

The examples of crack patterns after loading are shown in Figure 10. Only single crack is observed for PVA15 specimens. In most of PVA20 specimens, single crack between the notches and multiple cracks towards the loading points can be observed. It is considered that crack surfaces contact at final and compressive strut is formed.

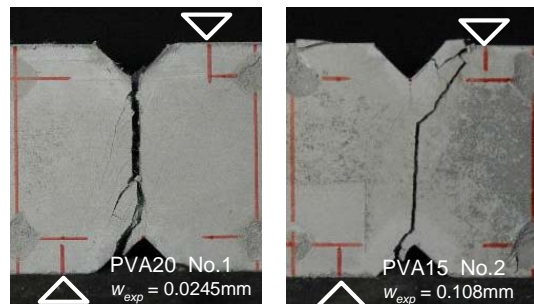


Figure 10. Examples of crack patterns after loading.

Shear stress versus axial deformation and shear deformation relationships of all specimens are

shown in Figure 11. Shear stress is normalized by the target tensile stress for each specimen. Shear stress is also revised to include  $P-\delta$  effect. In the PVA20 specimen, shear stress increases with a certain stiffness at the ratio of shear stress to the target tensile stress reaches to around 0.4, stiffness clearly increases with axial and shear deformation increase with constant shear stress. After that, in case of low level of target axial deformation (No.1 – No.4), shear stress starts to increase again at around 0.4mm of shear deformation. And then, shear stress shows the maximum and specimen fails. In case of large level of target axial deformation (No.5 – No.6), re-increment of shear stress after 0.4mm shear deformation can not be observed and specimen fails. In the PVA15 specimens, specimen fails at smaller deformation without re-increment of shear stress. The difference of fiber volume fraction causes clear difference of shear behavior.

Failure progress for ECC specimen can be explained as follows as shown in Figure 12;

**Stage I:**

Tensile loading starts. Tensile stress increases as an elastic manner.

**Stage II:**

First crack occurs. Tensile stress indicates first crack strength. Axial deformation increases with almost constant or slight increment of tensile stress. After reaching the target axial deformation ( $w_{exp}$ ), tensile stress keeps constant and shear loading starts.

**Stage III:**

Shear stress increases as almost elastic manner. If capacity for shear is small, specimen fails. (Branch a)

**Stage IV:**

Shear deformation increases with almost constant shear stress and tensile stress. If capacity for shear is not enough, specimen fails. (Branch b)

**Stage V:**

Crack surfaces contact and shear stress starts increasing again. Compressive strut via crack surface formed. After maximum shear stress, specimen fails by compression. (Branch c)

The test results are shown in Table 4. As a result, target axial deformation ranges from 0.02mm to 0.16mm and the target tensile stress (constant) is almost same as first crack strength. In

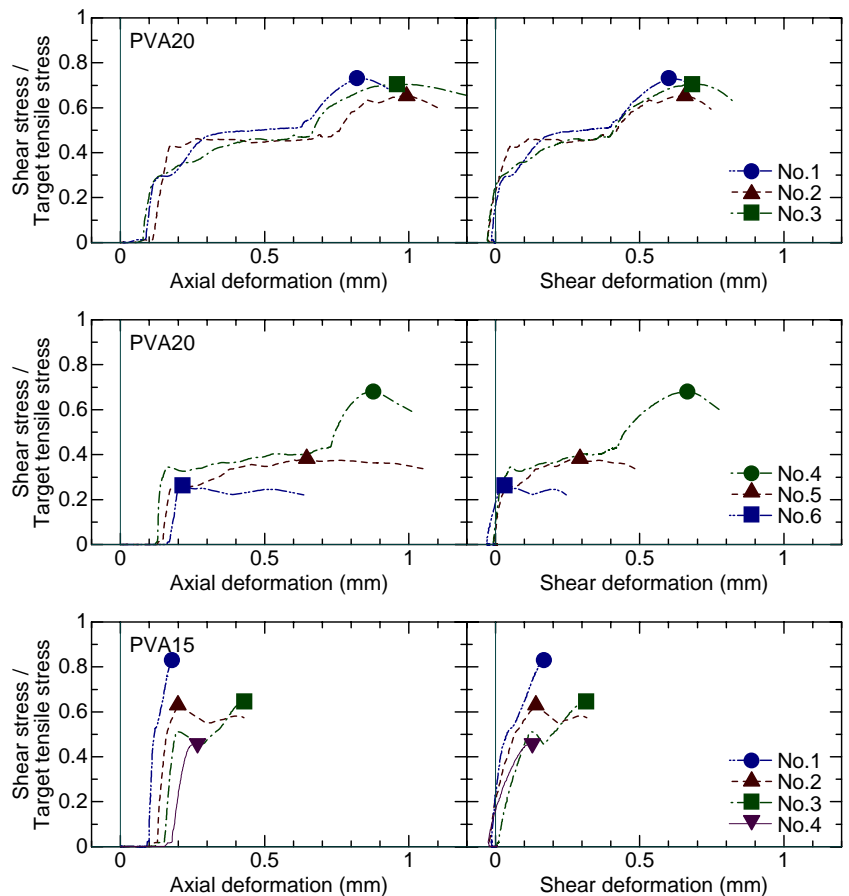


Figure 11. Shear stress – axial and shear deformation relationship.

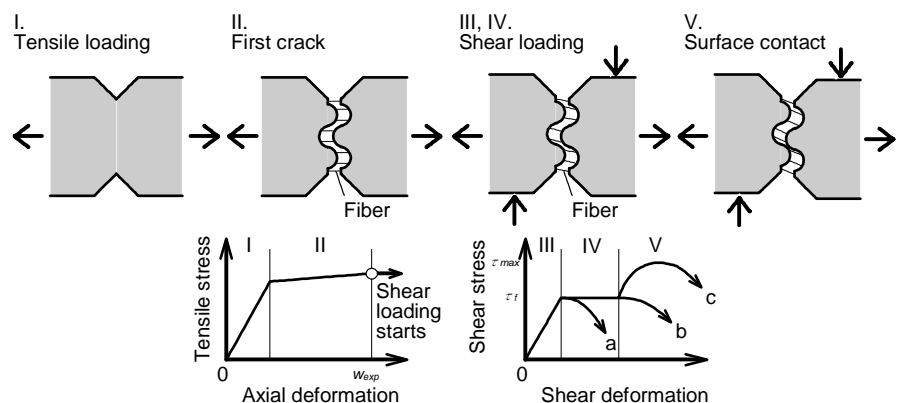


Figure 12. Failure progress of ECC specimen.

Table 4. Test results of ECC specimen.

ID	Target tensile stress $\sigma_{t,cons}$ (MPa)	Target axial deformation $w_{exp}$ (mm)	Tensile shear strength $\tau_f^*$ (MPa)	Shear strength $\tau_{max}$ (MPa)	
PVA20	No.1	3.58	0.0245	1.87	2.62
	No.2	3.86	0.0495	1.79	2.52
	No.3	3.84	0.0598	1.84	2.70
	No.4	4.25	0.121	1.73	2.89
	No.5	3.72	0.124	1.43	1.43
	No.6	4.28	0.161	1.13	1.13
PVA15	No.1	2.14	0.0918	1.15	1.78
	No.2	2.47	0.108	1.56	1.56
	No.3	2.44	0.122	1.25	1.57
	No.4	2.59	0.162	1.19	1.19

\* Shear stress at 'shear yielding'

indicate that normal stress for crack surface is possible to keep crack strength under shear.

### 3 PREDICTING METHOD FOR SHEAR CAPACITY OF ECC BEAMS

#### 3.1 Specimens for evaluation

Predicting method for shear capacity of steel reinforced (longitudinal bars and stirrups) ECC (R/ECC) beams is introduced. A small number of previous studies have been reported concerning shear testing for R/ECC beams. In this study, test results reported by the authors (Shimizu 2004 & 2005) are utilized to confirm predicting method for shear capacity. All beam specimens were tested by bending-shear loading (anti-symmetrical moment) as shown in Figure 13.

The list of specimens is shown in Table 5. Specimens have the 180 x 280mm size rectangular section, and shear span ratio ( $M/QD$ ) is 1.5 (L specimen) and 1.25 (S specimen). Arrangements of main bars and stirrups are D13 and D4 or D6. Parameters are fiber volume fraction ( $V_f$ ), shear span ratio, ratio of stirrup ( $p_w$ ) and yield strength of main bar ( $\sigma_y$ ). Fiber volume fraction of PVA fiber was set to 1.5 or 2.0%. Beam specimens named by the last alphabet of F are designed to have flexural

yielding before failure. Other specimens are designed to show shear failure before flexural yielding.

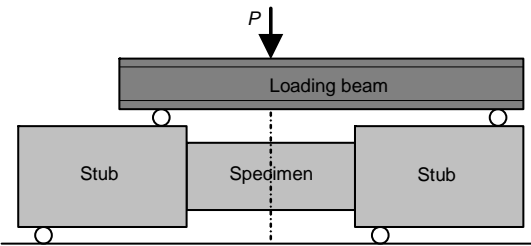


Figure 13. Loading method for R/ECC beam specimen.

Mechanical properties of PVA-ECC are shown in Table 6. Cylinder type test pieces with 100φ-200mm size are used for compression test. To determine the tensile characteristics of PVA-ECC, JCI Standard (JCI-S-003-2007) is adopted as described in Section 2.3.1.

#### 3.2 Outline of test results

The examples of crack patterns after loading are shown in Figure 14. Bending and shear crack are observed at 0.0025rad. The multiple cracks and restrain effect of crack opening could be observed. In shear failure type specimens, when load becomes around the maximum value, deformation was concentrated on a certain shear crack. The width of other

Table 5. List of R/ECC beam specimen.

ID	$V_f$ (%)	$M/QD$	$L$ (mm)	$b \times D$ (mm)	Main Bar Arrangement	$\sigma_y$ (MPa)	Stirrup Arrangement	$p_w$ (%)	$\sigma_{wy}$ (MPa)
PVA15-00L							-	0.00	-
PVA15-15L						719	2-D4@93	0.15	295
PVA15-30L		1.50	840				2-D4@47	0.30	
PVA15-60L	1.5					711	2-D6@59	0.60	
PVA15-89L									334
PVA15-89LF						438	2-D6@40	0.89	
PVA15-89S		1.25	700	180	8-D13	691	4-D6@59	1.20	427
PVA15-120S				x	$p_f=2.43\%$			0.00	-
PVA20-00L				280			-	0.00	-
PVA20-15L						719	2-D4@93	0.15	295
PVA20-30L		1.50	840				2-D4@47	0.30	
PVA20-60L	2.0					711	2-D6@59	0.60	
PVA20-89L									334
PVA20-89LF						438	2-D6@40	0.89	
PVA20-89S		1.25	700			691	4-D6@59	1.20	427
PVA20-120S									

Table 6. Mechanical properties of PVA-ECC.

Type	Compression			Tension*		Specimen for
	Elastic modulus (GPa)	Compressive strength (MPa)	Strain at strength (%)	Tensile strength (MPa)	Ultimate strain (%)	
PVA20	19.5	39.1	0.36	4.75	1.53	$p_w=0.00 - 0.30\%$ L
	19.5	45.8	0.39	4.33	0.67	$p_w=0.60 - 0.89\%$ L
	19.9	44.3	0.48	4.79	1.07	$p_w=0.89 - 1.20\%$ S
PVA15	16.3	35.7	0.35	3.83	1.02	$p_w=0.00 - 0.30\%$ L
	19.4	50.3	0.39	3.66	0.41	$p_w=0.60 - 0.89\%$ L
	17.4	42.0	0.42	2.41	0.43	$p_w=0.89 - 1.20\%$ S

\* Calculated value from bending test results (JCI-S-003-2007)

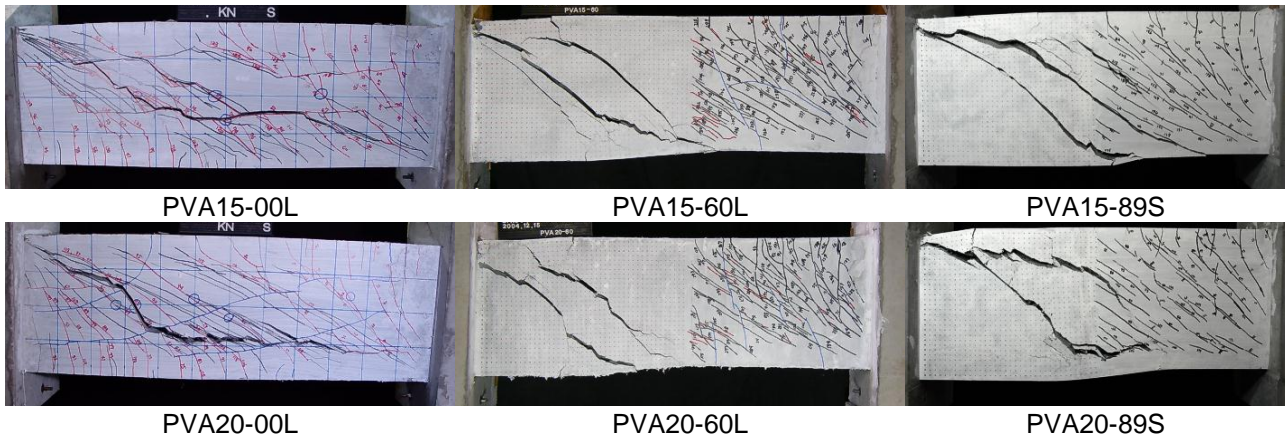


Figure 14. Crack pattern of R/ECC beam specimen after loading.

Table 7. Test results of R/ECC beam specimen.

ID	Translational angle ( $\times 10^{-3}$ rad) at		At maximum load		Ultimate angle <sup>*1</sup> ( $\times 10^{-3}$ rad)	Failure Mode <sup>*2</sup>
	Stirrup yielding	Main bar yielding	Shear force (kN)	Trans. angle ( $\times 10^{-3}$ rad)		
PVA15-00L	-	-	143	8.7	10.4	S
PVA15-15L	2.60	-	170	15.0	17.9	S
PVA15-30L	3.27	-	183	12.0	14.3	S
PVA15-60L	8.34	-	296	16.9	31.1	S
PVA15-89L	11.8	22.7	344	23.3	>50	F -> S
PVA15-89LF	13.1	10.8	270 <sup>*3</sup>	>50 <sup>*3</sup>	>50	F
PVA15-89S	8.36	-	296	17.5	46.0	S
PVA15-120S	7.34	-	344	22.0	56.1	S
PVA20-00L	-	-	183	10.6	12.6	S
PVA20-15L	-	-	206	12.8	15.2	S
PVA20-30L	5.50	-	209	19.0	22.6	S
PVA20-60L	11.1	-	310	18.8	23.9	S
PVA20-89L	11.5	19.2	341	19.2	43.1	F -> S
PVA20-89LF	11.6	10.8	272 <sup>*3</sup>	>50 <sup>*3</sup>	>50	F
PVA20-89S	9.43	-	337	16.6	38.6	S
PVA20-120S	9.23	19.7	406	23.9	44.9	F -> S

\*1 : Translational angle when load decreases to 80% of maximum. \*2 : S=Shear failure, F=Flexural yielding

\*3 : At the last point for deloading (1/20rad.)

cracks decreased due to localized deformation. The large difference between PVA15 and PVA20 specimen could not be recognized. In PVA15-89LF and PVA20-89LF specimens, load is in process of increasing when translational angle becomes 0.05rad. Main test results are listed in Table 7.

### 3.3 Evaluation of shear capacity

It is considered that principal tensile stress of ECC keeps tensile strength ( $\sigma_t$ ) at shear failure based on the knowledge from single plane shear test under tensile stress. The average of tensile stress on beam is expressed by  $\sigma_t$  with a reduction factor ( $\nu_t$ ). It is assumed that beam specimen exhibits the maximum load when compressive strut is failed by principal compressive stress. As a matter of fact, compressive failure at crack zone of beam specimen was recognized as shown in Figure 15. Because the compressive strut has some angles with main shear crack, local compressive failure takes place at the crack surface. This approach has same way to ordinary RC

beam. In case of RC, shear transmitting force at the crack surface is carried by mainly bearing action of coarse aggregate. In case of R/ECC, the force is carried by bridging action of fiber.

Based on the method of Architectural Institute of Japan for ordinary reinforced concrete beam (AIJ 1990), shear capacity of R/ECC beam is expressed as follows. This method is built up from the summation of the capacity of truss mechanism ( $V_t$ ), arch

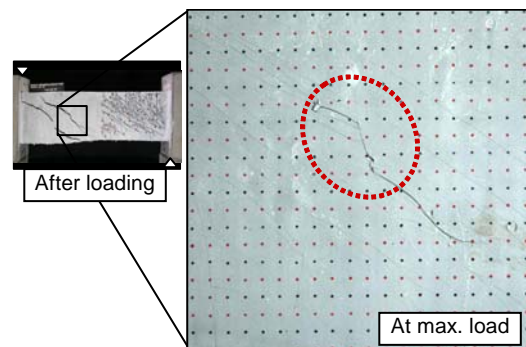


Figure 15. Local compression failure of R/ECC beam specimen.

mechanism ( $V_a$ ) and the effect of ECC ( $V_{ECC}$ ). The effective coefficient of compressive strength of ECC ( $\nu$ ) is treated as same as the case of ordinary concrete proposed by *fib*.

$$V = V_t + V_a + V_{ECC} \quad (4)$$

$$V_t = b \cdot j_t \cdot p_w \cdot \sigma_{wy} \cdot \cot \phi \quad (5)$$

$$V_a = \tan \theta \cdot (1 - \beta) \cdot \nu \cdot \sigma_B \cdot b \cdot D / 2 \quad (6)$$

$$\tan \theta = \sqrt{(L/D)^2 + 1} - (L/D) \quad (7)$$

$$\beta = (1 + \cot^2 \phi) \cdot p_w \cdot \sigma_{wy} / \nu \cdot \sigma_B \quad (8)$$

$$\nu = 1.70 \sigma_B^{-0.333} \quad (9)$$

$$\cot \phi = \min \left\{ \begin{array}{l} 2.0 \\ j_t / (D \cdot \tan \theta) \\ \sqrt{\nu \cdot \sigma_B / (p_w \cdot \sigma_{wy})} - 1 \end{array} \right. \quad (10)$$

$$V_{ECC} = b \cdot j_t \cdot \nu_t \cdot \sigma_t \cdot \cot \phi \quad (11)$$

where,

$V$  = shear capacity

$V_t$  = shear capacity by truss mechanism

$V_a$  = shear capacity by arch mechanism

$b$  = width of member

$j_t$  = distance between compression and tension bars

$p_w$  = stirrup ratio

$\sigma_{wy}$  = yield strength of stirrup

$\sigma_B$  = compressive strength of ECC

$\phi$  = angle of compressive strut

$\theta$  = angle of arch mechanism

$\nu$  = effective coefficient of compressive strength of ECC

$D$  = depth of member

$L$  = clear span length

$\nu_t$  = reduction factor for tensile strength of ECC

$\sigma_t$  = tensile strength of ECC

Reduction factor for tensile strength of ECC ( $\nu_t$ ), which may express the uniformness of tensile stress on the crack surface, is unknown. In this study, 0.5 is adopted. The experimental value of maximum shear force by R/ECC beam specimen is plotted with calculated shear capacity in Figure 16. Both maximum shear force and calculated shear capacity is standardized by calculated bending strength in shear force. The experimental values show good agreement with calculated values. The average of the ratios of experimental values to calculated shear capacity for shear failure type specimens is 1.09.

## 4 CONCLUSIONS

The method of single plane shear test under tensile stress as normal stress on crack surface is newly de-

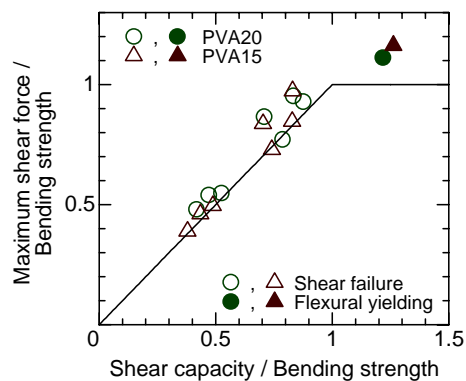


Figure 16. Comparison between calculated shear capacity and experimental one.

veloped to clarify shear transfer mechanism on crack surface of ECC. From the test results, shear strength on crack surface is about half of tensile strength. This means that normal stress for crack surface is possible to keep crack strength under shear. Predicting method for shear capacity of R/ECC beams is proposed based on the arch-truss method with the summation of the effect of ECC. The effect is expressed by multiplying the reduction factor (0.5) to tensile strength obtained from the evaluation of tensile properties using bending test. The experimental values show good agreement with calculated ones.

## ACKNOWLEDGEMENT

The authors acknowledge the kind support of Koken Sangyo Co. Ltd. for producing the specimens.

## REFERENCES

- Architectural Institute of Japan (AIJ). 1990. Design Guidelines for Earthquake Resistant Reinforced Concrete Buildings Based on Ultimate Strength Concept, pp.106-116.
- Japan Concrete Institute (JCI) Standard. 2007. Method of test for bending moment-curvature curve of fiber-reinforced cementitious composites JCI-S-003-2007, [http://www.jci-web.jp/jci\\_standard/img/JCI-S-003-2007-e.pdf](http://www.jci-web.jp/jci_standard/img/JCI-S-003-2007-e.pdf).
- Kanakubo, T. 2006. Tensile Characteristics Evaluation Method for Ductile Fiber-Reinforced Cementitious Composites, Journal of Advanced Concrete Technology, Vol.4, No.1, pp.3-17.
- Li, H., Maekawa, K. & Okamura, H. 1990. Shear Transfer Mechanism on Reinforced Concrete Crack Surface, Proceedings of Japan Concrete Institute, Vol.12, No.2, pp.293-298.
- Mattcock, A.H. & Howkins, N.M. 1972. Shear Transfer in Reinforced Concrete Recent Research, PCI Journal, Vol.17, No.2, pp.55-75.
- Shimizu, K., Kanakubo, T., Kanda, T. & Nagai, S. 2004. Shear Behavior of Steel Reinforced PVA-ECC Beams, 13th World Conference on Earthquake Engineering, Conference Proceedings DVD, Paper No. 704.
- Shimizu, K., Kanakubo, T., Kanda, T. & Nagai, S. 2005. Shear Behavior of PVA-ECC Beams, International RILEM Workshop on High Performance Fiber Reinforced Cementitious Composites in Structural Applications, RILEM Proceedings PRO 49, pp.443-451.